Performance Prediction of Rotary Desiccant Wheel

Y. Momoi
Osaka University
R. Yoshie
Tokyo Polytechnic University
A. Satake
Maeda Corporation
H. Yoshino
Tohoku University

ABSTRACT

In the desiccant dehumidifier using adsorbent such as silica gel and zeolite, outdoor moist air is dehumidified in adsorbent. On the other hands, it is necessary for the adsorbent which becomes moist by dehumidifying outdoor air to be dried (regenerated). Utilizing solar thermal energy as a heat source for the regeneration of the adsorbent leads to large energy conservation. In order to spread the heating and hot-water supply systems that utilize solar heat, it is one key to find how to use the surplus solar heat during summer, spring, and autumn seasons. Therefore, we are developing a wheel-type solid desiccant cooling system using this surplus solar heat. We aim to develop the highly efficient desiccant cooling system using solar thermal energy and investigated a numerical method which simulates combined heat and moisture transfer processes inside a rotary desiccant wheel. The desiccant wheel is the main component of a solid desiccant cooling system.

In this paper, firstly, mass transfer coefficient that has a great influence on the dehumidification performance of the desiccant wheel was derived from the experimental results. It is clarified that the mass transfer coefficient becomes smaller with the decrease in the rotational speed. Secondly, temperature and humidity of the air that has passed through the desiccant wheel were predicted using our numerical method, and the validity of this method was examined by comparing calculation results with measurement results. Finally, the optimum rotational speed with changing the diameter of the desiccant wheel was discussed, using the numerical model.

1. INTRODUCTION

In order to promote the utilization of solar heat for hot-water supply and air-conditioning systems, the authors have started the research and development of a wheel-type solid desiccant cooling system that utilizes surplus solar heat, which emerges in summers, springs, and autumns, for regenerating the adsorbent. In order to develop a highly efficient desiccant system utilizing solar heat, we are examining the pre-cooling technique of the adsorbing part of the desiccant wheel, unique post-cooling methods, and the application of new adsorbing materials. We also intend to optimize a variety of parameters that affect the performance of the desiccant cooling system. There are a large number of parameters that determine the performance of a desiccant system such as desiccant material's moisture adsorption/desorption characteristics, size of the wheel, air volume, process/regeneration splitting ratio, rotational speed, temperature of regeneration, porosity, and the degree of pre-cooling. Accordingly, it costs an enormous amount of time and labor to find the appropriate combination of parameters by experiment.

Therefore, we developed a technique for numerical analysis of heat and moisture transfers, considering the rotation of a desiccant wheel in order to carry out the optimum design of a desiccant cooling system. The heat and moisture transfer phenomenon inside a desiccant wheel was formulated, and the algorithm of numerical calculation for the formulated equations was investigated. In addition, we measured equilibrium moisture content, adsorption and desorption heats, and

mass transfer coefficient of the desiccant wheel which are very important parameters for the dehumidification performance and are used as input data for the numerical analysis. Then we discuss the validity of the numerical method by comparing the numerical analysis results with experimental results.

2. NUMERICAL METHOD

2.1 Heat and Water Vapor Transport Equations

As shown in Fig. 1, a parallelepiped infinitesimal is taken from a cylindrical honeycomb wheel, to produce a model of heat and moisture transfers inside a desiccant wheel. By assuming that the flow direction is the x-direction and that pressure and flow rate are constant, and considering the balances of water vapor and heat inside this infinitesimal volume, the following three 1-demensional transport equations (1), (2), and (3) cab be obtained:

$$\varepsilon\rho_a \frac{\partial X_a}{\partial t} = -\varepsilon u \rho_a \frac{\partial X_a}{\partial x} + \varepsilon \frac{\partial}{\partial x}\left(\lambda_a' \frac{\partial X_a}{\partial x}\right) - \gamma \frac{\partial w}{\partial t} \quad (1)$$

$$\varepsilon C_a \rho_a \frac{\partial \theta_a}{\partial t} = -\varepsilon u \rho_a C_a \frac{\partial \theta_a}{\partial x} + \varepsilon \frac{\partial}{\partial x}\left(\lambda_a \frac{\partial \theta_a}{\partial x}\right) - \alpha S\left(\theta_a - \theta_d\right) \quad (2)$$

$$(1-\varepsilon) C_d \rho_d \frac{\partial \theta_d}{\partial t} = (1-\varepsilon)\frac{\partial}{\partial x}\left(\lambda_d \frac{\partial \theta_d}{\partial x}\right) + L\alpha' S\left(X_a - X_b\right) + \alpha S\left(\theta_a - \theta_d\right) \quad (3)$$

In addition, the adsorption speed equation can be expressed by Equation (4), considering the moisture transfer driven by the difference in absolute humidity between the surface of the desiccant material and the air of the flow.

$$\gamma \frac{\partial w}{\partial t} = \alpha' S\left(X_a - X_b\right) \quad (4)$$

The relation between the absolute humidity and the moisture content on the surface of the desiccant material can be expressed by Equation (5), under the assumption of the local equilibrium that the relation immediately follows the equilibrium water content curve.

$$w = f\left(X_a, \theta_a\right) = f\left(X_b, \theta_d\right) \quad (5)$$

where:

ε is porosity (ratio of the air passage area to the cross-sectional area of a wheel) [-], ρ_a is air density [kg/m^3], ρ_d is desiccant material density [kg$_d$/m^3], X_a is the absolute humidity of flow passage air [kg/kg'], X_b is the absolute humidity of adsorption layer (desiccant material surface) [kg/kg'], t is time [s], x is the coordinate in the direction of the air passage axis, u is air velocity [m/s], λ_a' is the moisture conductivity of air [kg/sm(kg/kg')], λ_d' is the moisture conductivity of desiccant material [kg/sm(kg/kg')], γ is the filling density of desiccant material (the mass of desiccant material per unit volume including the air passage) [kg$_d$/m^3], w is moisture content (water vapor adsorption amount per unit mass of desiccant material) [kg/kg$_d$], α' is the moisture transfer coefficient on desiccant material surface [kg/sm^2(kg/kg')], α is the heat transfer coefficient on desiccant material surface [J/sm^{2}K], S is the desiccant material surface area per unit volume including the air passage [m^2/m^3], C_a is the specific heat of air [J/kgK], C_d is the specific heat of desiccant material [J/kgK], θ_a is the temperature of passage air [^{o}C], θ_d is the temperature of desiccant material [^{o}C], λ_a is the thermal conductivity of air [J/smK], λ_d is the thermal conductivity of desiccant material [J/smK], and L is adsorption/desorption heat [J/kg].

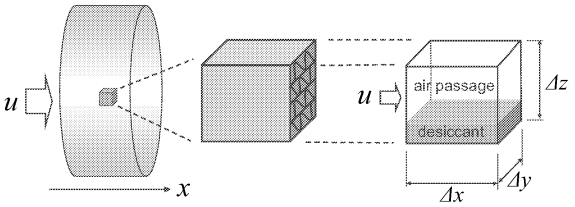

Fig. 1: Modeling of desiccant wheel.

2.2 Algorithm

The above 5 equations are spatially discretized in the flow direction based on the control volume method, to calculate 5 unknown values: X_a, X_b, θ_a, θ_d, and w. The algorithm is that each variable is set at an initial value, then Equations (1), (2), (3), and (4) are solved with the full implicit scheme using the tridiagonal matrix algorithm (TDMA; Patankar, 1980), to obtain the tentative values of X_a, θ_a, θ_d, and w at the next time step, and then a convergent calculation between Equations (4) and (5) is carried out to determine the tentative w and X_b. Using these updated tentative values, the above procedures are repeated with the Gauss-Seidel method until convergence, to determine the

values at the next time step. When the values at the next time step are determined, the time step proceeds to the next one.

In the numerical analysis considering the rotation of a wheel, the wheel is divided into independent segments in the rotational direction, as shown in Fig. 2, and then the above calculation is carried out for each divided segment independently. Each segmented element is rotated, and the flow direction and the inflow temperature and humidity are switched, according to whether it is located at the adsorption side or the desorption side. By averaging the outflow temperature and humidity of all elements located at the adsorption side, it is possible to obtain the temperature and humidity of the air that has been dehumidified through the wheel at each time step. Until this averaged temperature and humidity become steady, the calculation is continued while rotating the wheel.

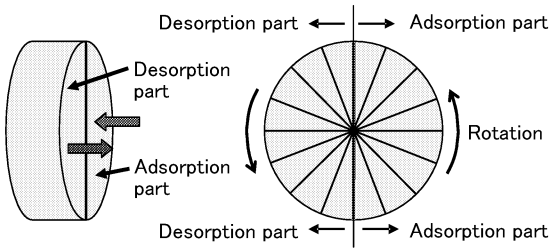

Fig. 2: Numerical analysis of rotating wheel.

3. MEASUREMENT OF ADSORPTION / DESORPTION HEATS AND MASS TRANSFER COEFFICIENT

Fig. 3 shows experimental apparatus. The wheel was covered with thermal insulation and set on an electronic balance. Process air and regeneration air were sent from one direction and switched by a manual switching damper. The mass changes of the desiccant wheel in the adsorption and desorption processes were directly measured by the electric balance. In addition, the temperature and humidity at the upstream and downstream sides of the wheel were measured simultaneously. The experimental conditions are shown in Table 1. In isothermal experiment, the process air has high humidity and the regeneration air has low humidity, while both temperatures are 25 °C. Adsorption and desorption heats are calculated from the temperature change of the air that has passed through the wheel. In the heating-regeneration experiment, the regeneration-side air was heated to 70 °C, measurement was carried out with changing the interval of switching dampers, considering wheel rotation.

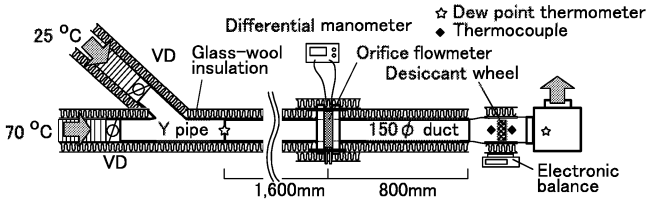

Fig. 3: Experimental apparatus.

Table 1: Experimental condition.

	Isotherm	Heating-regeneration
Process air temperature and humidity	25 °C 17.5 g/kg'	25 °C 9 g/kg'
Regeneration air temperature and humidity	25 °C 5 g/kg'	70 °C 9 g/kg'
Airflow rate (Velocity)	100 m^3/h (2.2 m/s)	104.4 m^3/h (2.32 m/s)
Switching interval	Until adsorption/ desorption equilibrium	Until adsorption/ desorption equilibrium, every 1 min, 1.5 min, 3 min and 6 min

3.1 Isothermal Experiment

Fig. 4 shows the change of the water content of the desiccant wheel. The mass changed by about 64 g, and the moisture content changed by 0.12 kg/kg_d. Fig. 5 shows the results of temperature measurements at the upstream and downstream sides of the wheel. Adsorption/desorption heat L [J/kg] was calculated with the following equation, from the adsorption amount ΔW [kg] obtained through the measurement (see Fig. 4) and the temperature difference between the upstream and downstream sides of the wheel $\Delta\theta$ ($= \theta_1 - \theta_2$) [K] (see Fig. 5).

$$L = \frac{\int C_a \rho_a Q \Delta\theta \, \mathrm{d}t}{\Delta W} \qquad (6)$$

where: Q represents airflow rate [m^3/s].

Table 2 shows the calculated adsorption and desorption heats. Both heats were larger than the evaporative latent heat of water (= 2.44 MJ/kg at 25 °C). This is because the force of attraction between adsorbent and a water molecule is stronger than the force of attraction between water molecules in the liquid state. This result is consistent with the simplified equation (Barlow, 1982).

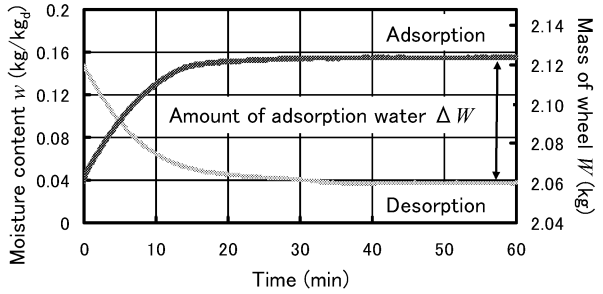

Fig. 4: Water content of desiccant wheel.

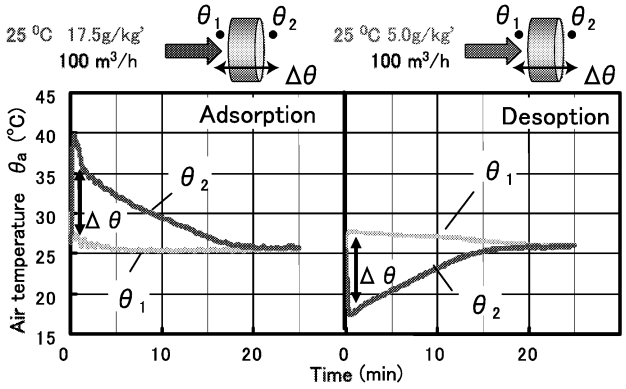

Fig. 5: Temperature of Air through desiccant wheel.

Table 2: Calculation of adsorption and desorption heat.

Adsorption heat	2.75 MJ/kg
Desorption heat	2.95 MJ/kg

3.2 Heating Regeneration Experiment

Mass transfer coefficient α'S in the Equation (4) considerably influences the adsorption amount when the adsorbent repeats adsorption and desorption. This mass transfer coefficient α'S was estimated from experiment, as follows. In Equation (4), the time variation of moisture content dw/dt in the left-hand side can be obtained from the gradient shown in Fig. 4. The absolute humidity of the inlet air X_a in the right-hand side of Equation (4) can be directly obtained from the measurement. Therefore, if the absolute humidity of the adsorption layer X_b is known, it is possible to calculate α'S. However, it is difficult to measure X_b directly. Accordingly, in Equation (5), it is assumed that the temperature of desiccant material θ_d is equal to the average of the upstream and downstream sides of the air temperatures, and X_b is estimated from θ_d and moisture content w. This assumption is not inappropriate because the thickness of the desiccant material is so thin (0.2 mm) and its both surfaces is exposed to the passage air that the temperature of the desiccant material is almost equal to the passage air.

Figs. 6 and 7 show α'S calculated with the above mentioned method at 10 sec intervals after the start of adsorption/desorption. α'S decreased with time. This is because the adsorption speed is determined by the transfer rate inside the film on the adsorbent surface and the diffusion speed in fine pores, and as for porous material, the resistance for the intra-pore diffusion increases as the adsorption amount increases, and so the intra-pore diffusion becomes dominant (the slow adsorption speed limits the entire adsorption speed), and then the adsorption speed decreases. The damper switching interval was converted into the rotational speed of the wheel (For example, the 6 min interval means 6 minutes of adsorption and 6 minutes of desorption, that is, a total 12 minutes, and so this corresponds to a rotational speed of 5 revolution per hour).

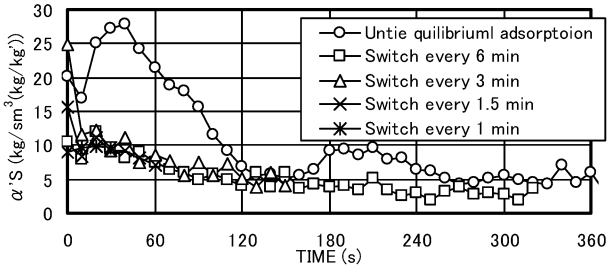

Fig. 6: Mass transfer coefficient in adsorption.

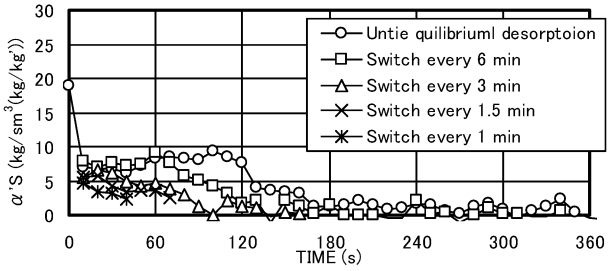

Fig. 7: Mass transfer coefficient in desorption.

4. RESULTS AND DISCUSSIONS

4.1 Comparison between Adsorption/Desorption Experiment and Numerical Analysis

In order to validate the numerical calculation method, we compared the calculation results with the experimental results for an actual desiccant machine. In the calculation, a desiccant wheel with a diameter of 0.3 m and

depth of 0.1 m was divided into 20 cells in the flow direction. The calculation was carried out at 0.1 sec intervals. The temperatures and absolute humidities of the process-side and regeneration-side air were set to be equal to experimental values: 30 °C, 14.7 g/kg', 70 °C, and 10.7 g/kg', respectively. The calculation was continued until the results became periodic steady state. $\alpha' S$ was set so that it becomes small when rotational speed is low as shown in Fig. 8. However, the above mentioned experiment has a problem in the measurement precision when rotational speed is high, and so α'S was set based on trial and error. In addition, the experiment results (Yoshie, 2007) shown in Fig. 9 were used for the equilibrium moisture content curve in Equation (5). The other calculation conditions are shown in Table 3.

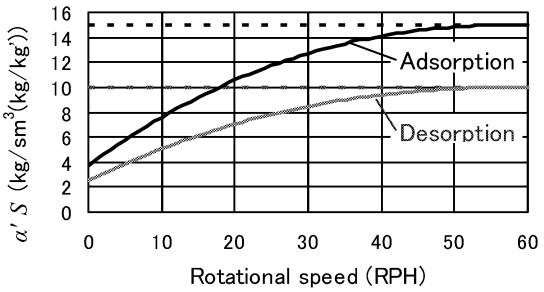

Fig. 8: Adsorption/desorption speed.

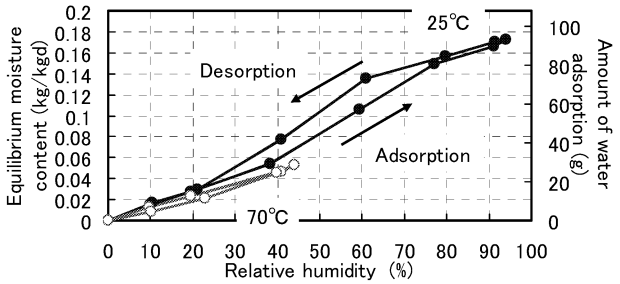

Fig. 9: Adsorption/desorption isotherm.

Table 3: Calculation condition.

ε =0.71, ρ_d =988 kg/m^3, α =60 J/sm^{2}K, u =1.16 m/s, λ' =0.000032 kg/ms(kg/kg'), S =2925 m^2/m^3, γ =289 kgd/m^3, L =2.85 MJ/kg, C_a =1006 J/kgK, C_d =580 J/kgK, λ_a =0.022 J/smK, λ_d =1.0 J/smK

The dehumidification performance is evaluated by adsorption speed MRC and desorption speed MRR, which are defined by follows.

$$MRC = \dot{m}_{pro}\left(X_{OA} - X_{SA}\right)\times 3600 \text{ (kg/hr)} \qquad (7)$$

$$MRR = \dot{m}_{reg}\left(X_{EA} - X_{RA}\right)\times 3600 \text{ (kg/hr)} \qquad (8)$$

where:

$\dot{m}_{pro}$ represents the mass flow rate of process-side air [kg/s], $\dot{m}_{reg}$ represents the mass flow rate of regeneration-side air [kg/s], X_{OA}, X_{SA}, X_{RA}, and X_{EA} denote the absolute humidities of the air at the process-side inlet, the process-side outlet, the regeneration-side inlet, and the regeneration-side outlet, respectively. As the MRC and the MRR are larger, the water adsorption/desorption amount per unit time increases, and so it can be said that the dehumidification performance is high. Figs. 10 and 11 show the temperatures and absolute humidities of the air at the process-side outlet (SA) and the regeneration-side outlet (EA). The calculated temperatures and humidities correspond well with the experimental ones.

Figs. 12 and 13 show the comparison between the experimental and calculation results for the MRC and the MRR. The calculation predicted the MRC and MRR within an accuracy of 5 % for all the rotational speed conditions.

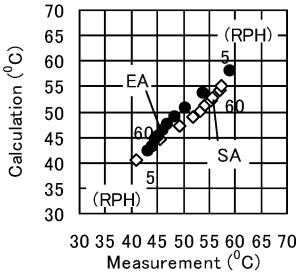

Fig. 10: Temperature Comparison.

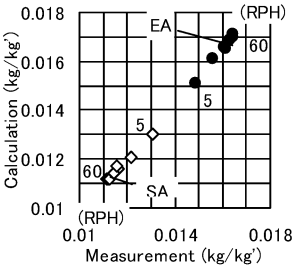

Fig. 11: Absolute humidity comparison.

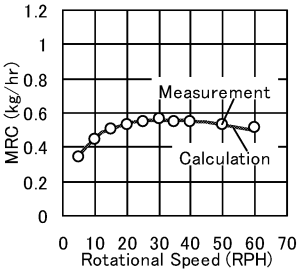

Fig. 12: MRC.

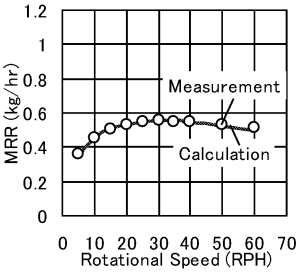

Fig. 13: MRR.

4.2 Optimum Rotational Speed of Wheel

The optimum rotational speeds for various wheel diameters were investigated using the numerical analysis. Here, optimum rotational speed was defined as the rotational speed at

which MRC becomes the maximum. The calculation was carried for D = 0.2 m, 0.3 m, 0.4 m, and 0.6 m. The flow rate was fixed at 100 m^3/h for every case. The flow velocity determined by this flow rate and the air passage area were given at the inlet boundary for the numerical analysis. The values other than flow velocity were the same as those in Table 3.

Fig. 14 shows the calculated MRC. When D = 0.2 m, the optimum rotational speed was 48 RPH, which is higher than 32 RPH: the value when D = 0.3 m. When D = 0.2 m, the specified air velocity is high, and the flow volume per air passage and unit time is large, and so the inlet water vapor content is large. Therefore, adsorption equilibrium is reached earlier, and so it is better to change adsorption and desorption processes rapidly by increasing rotational speed. Meanwhile, when wheel's diameter is increased, airflow rate decreases, and adsorption equilibrium takes longer time, and so it is better that the rotational speed of the wheel is low.

Fig. 15 shows the plotted optimum rotational speed, with the horizontal axis representing air velocity through air passage of the wheel, for each wheel diameter. This figure indicates that as air velocity increases, optimum rotational speed also increases. As long as the wheel's material and thickness are the same, even if airflow rate and wheel's diameter are different, it is possible to estimate the optimum rotational speed, using the air velocity and the curve shown in Fig. 15.

5. CONCLUSIONS

The heat and moisture transfer phenomena inside a desiccant wheel were formulated, and its numerical simulation method was developed. In order to obtain the adsorption and desorption heats and mass transfer coefficient which are necessary for the numerical simulation, experiments of repeating adsorption and desorption were conducted. The experimental results showed that the mass transfer coefficient decreases with time after the start of adsorption/desorption. Numerical analysis considering this decrease in the mass transfer coefficient was carried out and the results were compared with experimental results to validate the numerical simulation method. The temperature and humidity at the wheel outlet and adsorption and desorption speeds obtained by the numerical analysis were almost the same as those of the experiments. In addition, numerical analysis was conducted changing the air velocity through the wheel, and it was clarified that as the air velocity increases, the optimum rotational speed increases.

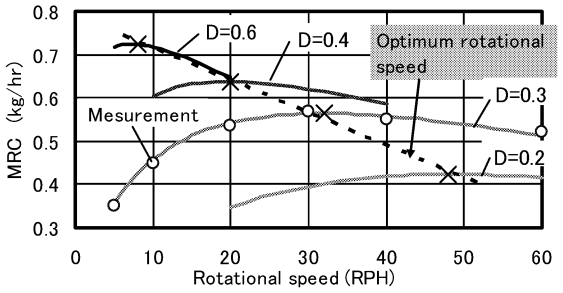

Fig. 14: MRC with desiccant wheel's diameter.

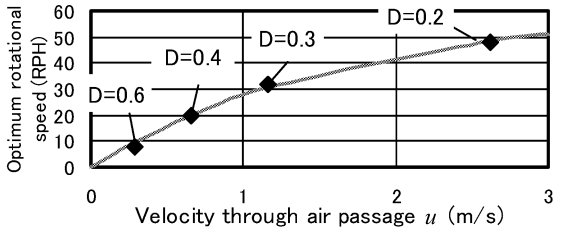

Fig. 15: Optimum rotational speed of the wheel.

ACKNOWLEDGEMENT

The authors gratefully acknowledge the New Energy and Industrial Technology Development Organization (NEDO) of Japan through the Project of Solar Energy and New System Technology Resources and Development for funding this research with contract number 05002503-0. Research members include Prof. Mochida, Dr. Takaki, Dr. Lun, Dr. Yonekura, Mr. Enteria (Tohoku University), Mr. Kawahara, Mr. Kubo (Maeda Corporation), Dr. Mitamura (Ashikaga Institute of Technology) and Mr. Baba (Earth Clean Tohoku).

REFERENCES

Patankar, S.V. (1980). Numerical Heat Transfer and Fluid Flow, *Hemisphere Publ. Corp.*

Barlow, R.S. (1982). Analysis of the Adsorption Process and of Desiccant Cooling Systems. - A Pseudo-Steady-State Model for Coupled Heat and Mass Transfer, *SERI/TR-631-1330*.

Yoshie, R., Momoi, Y., Satake, A., Yoshino, H. and Mitamura, T. (2007). Numerical Analysis of Heat and Moisture Transfer in Desiccant Wheel for Dehumidification, *Proceedings of Clima 2007 WellBeing Indoors Abstract Book*: p.531